Role of the $N^*(2080)$ in $pp \to pK^+\Lambda(1520)$ and $\pi^- p \to K^0\Lambda(1520)$ reactions

Ju-Jun Xie[1, 2, *] and Bo-Chao Liu[3, 2, †]

[1] *Institute of Modern Physics, Chinese Academy of Sciences, Lanzhou 730000, China*
[2] *State Key Laboratory of Theoretical Physics, Institute of Theoretical Physics, Chinese Academy of Sciences, Bejing 100190, China*
[3] *Department of Applied Physics, Xi'an Jiaotong University, Xi'an, Shanxi 710049, China*

We investigate the $\Lambda(1520)$ hadronic production in the $pp \to pK^+\Lambda(1520)$ and $\pi^- p \to K^0\Lambda(1520)$ reactions within the effective Lagrangian method. For $\pi^- p \to K^0\Lambda(1520)$ reaction, in addition to the "background" contributions from $t-$channel K^* exchange, $u-$channel Σ^+ exchange, and $s-$channel nucleon pole terms, we also consider the contribution from the nucleon resonance $N^*(2080)$ (spin-parity $J^P = 3/2^-$), which has significant coupling to $K\Lambda(1520)$ channel. We show that the inclusion of the nucleon resonance $N^*(2080)$ leads to a fairly good description of the low energy experimental total cross section data of $\pi^- p \to K^0\Lambda(1520)$ reaction. From fitting to the experimental data, we get the $N^*(2080)N\pi$ coupling constant $g_{N^*(2080)N\pi} = 0.14 \pm 0.04$. By using this value and with the assumption that the excitation of $N^*(2080)$ is due to the π^0-meson exchanges, we calculate the total and differential cross sections of $pp \to pK^+\Lambda(1520)$ reaction. We also demonstrate that the invariant mass distribution and the Dalitz Plot provide direct information of the $\Lambda(1520)$ production, which can be tested by future experiments.

PACS numbers: 13.75.-n.; 14.20.Gk.; 13.30.Eg.

I. INTRODUCTION

The study of hadron structure and the spectrum of hadron resonance is one of the most important issues in hadronic physics and is attracting much attention (see Ref. [1] for a general review). In past decades, many excited states of baryon were observed and their properties have been measured [2]. For those nucleon resonances with mass below 2.0 GeV, most of their parameters, such as mass, total decay width, decay modes, etc., have been more or less studied both on experimental and theoretical sides. However, for the states around or above 2.0 GeV, our present knowledge on them is still in its infancy [2]. Moreover there are still many theoretical predictions of "missing N^* states" around 2.0 GeV, which have not so far been observed [3]. Since more number of effective degree of freedoms will induce more predicted number of excited states, the "missing N^* states" problem is in favor of the diquark configuration which has less degree of freedom and predicts less N^* states [4]. So, studying the nucleon resonances around or above 2.0 GeV, not only on experimental side but also on theoretical side, is interesting and needed.

The associated strangeness production reaction, $pp \to pK^+\Lambda(1520)$, is interesting. Firstly, this reaction requires the creation of an $s\bar{s}$ quark pair. Thus, a thorough and dedicated study of strangeness production mechanism in this reaction has the potential to gain a deeper understanding of the interaction among strange hadrons and also on the nature of baryon resonances. Secondly, it is a good channel to study the N^* resonances around 2.0 GeV which have significant couplings to $K\Lambda(1520)$ channel, because the $K\Lambda(1520)$ is a pure isospin 1/2 channel and the production threshold of $K\Lambda(1520)$ is about 2.0 GeV. Thirdly, the near threshold differential and total cross sections for kaon pair production in the $pp \to ppK^+K^-$ reaction have been measured by DISTO Collaboration [5], COSY-11 Collaboration [6, 7], and COSY-ANKE Collaboration [8–10]. These results show clear evidence for the excitation and decay of ϕ meson sitting on a smooth K^+K^- background. For the non-ϕ kaon pair production, the role of the low energy Λ excited state, $\Lambda(1405)$, have been studied in Ref. [11] by using chiral unitary theory and in Ref. [12] within an unified approach using an effective Lagrangian model. Since the $\Lambda(1405)$ state lies below K^-p threshold, it is expected to give significant contribution at the energies near the threshold. But, at higher energies, the next Λ excited state, $\Lambda(1520)$, could be important for the non-ϕ kaon pair production in the $pp \to pK^+\Lambda(1520) \to pK^+K^-p$ reaction.

In Refs. [13–15], the contribution from a nucleon resonance with spin-parity $3/2^-$ and mass around 2.1 GeV was studied in the $\Lambda(1520)$ ($\equiv \Lambda^*$) photo- or electroproduction processes. They all found that this nucleon resonance has a significant coupling to $K\Lambda(1520)$ channel and plays an important role in these reactions. Before the 2012 Particle Date Group (PDG) review, this nucleon resonance was filed as a two-star nucleon resonance $N^*(2080)$, which is now named as $N^*(2120)$ [2] [1].

In the present work, we study the role of $N^*(2080)$ resonance ($\equiv N^*$) in the $pp \to pK^+\Lambda(1520)$ and $\pi^- p \to K^0\Lambda(1520)$ reactions within the effective Lagrangian method. Unfortunately, the information about $N^*(2080)$

* xiejujun@impcas.ac.cn
† liubc@xjtu.edu.cn

[1] In order for convenience, here after, we still call it as $N^*(2080)$.

resonance is scarce [2] and the knowledge of its properties, like mass, total decay width, branch ratios, are poor. In this work, we take its mass and total decay width as 2115 MeV and 254 MeV, respectively, which are obtained by fitting them to the experimental data on the $\gamma p \to K^+\Lambda(1520)$ reaction in Ref. [13]. For the $N^*(2080)K\Lambda(1520)$ coupling constant, we also take the value that was obtained in our previous work [13]. Finally, from fitting to the experimental data of $\pi^- p \to K^0\Lambda(1520)$ reaction, we can get the $N^*(2080)N\pi$ coupling constant, then we study the role of $N^*(2080)$ resonance in the $pp \to pK^+\Lambda(1520)$ reaction with the assumption that the production mechanism is solely due to the π^0-meson exchange.

In the next section, we will give the formalism and ingredients in our calculation, then numerical results and discussions are given in Sect. III. A short summary is given in the last section.

II. FORMALISM AND INGREDIENTS

The combination of effective Lagrangian method and isobar model is an important theoretical approach in describing the various processes in resonance production region. In this section, we introduce the theoretical formalism and ingredients to calculate the $\Lambda(1520)$ hadronic production in $\pi^- p \to K^0\Lambda(1520)$ and $pp \to pK^+\Lambda(1520)$ reactions within the effective Lagrangian method.

A. Feynman diagrams and interaction Lagrangian densities

The basic tree level Feynman diagrams for the $\pi^- p \to K^0\Lambda(1520)$ and $pp \to pK^+\Lambda(1520)$ reactions are depicted in Fig. 1 and Fig. 2, respectively. For the $\pi^- p \to K^0\Lambda(1520)$ reaction, in addition to the "background" diagrams, such as $t-$channel K^* exchange, $u-$channel Σ^+ exchange, and $s-$channel nucleon pole diagrams, we also consider the $s-$channel $N^*(2080)$ resonance excitation process. While for the $pp \to pK^+\Lambda(1520)$ reaction, the $t-$channle K^* exchange process is neglected since its contribution is small, which will be discussed below.

For the $\pi^- p \to K^0\Lambda(1520)$ reaction, to compute the contributions of those terms shown in Fig. 1, we use the interaction Lagrangian densities as in Refs. [13, 16–24],

$$\mathcal{L}_{\pi NN} = ig_{\pi NN}\bar{N}\gamma_5\vec{\tau}\cdot\vec{\pi}N, \tag{1}$$

$$\mathcal{L}_{KN\Lambda^*} = \frac{g_{KN\Lambda^*}}{m_K}\bar{\Lambda}^{*\mu}(\partial_\mu K)\gamma_5 N + \text{h.c.}, \tag{2}$$

$$\mathcal{L}_{\pi NN^*} = \frac{g_{\pi NN^*}}{m_\pi}\bar{N}^{*\mu}\gamma_5(\partial_\mu\vec{\tau}\cdot\vec{\pi})N + \text{h.c.}, \tag{3}$$

$$\mathcal{L}_{K\Lambda^*N^*} = \frac{g_1}{m_K}\bar{\Lambda}^*_\mu\gamma_5\gamma_\alpha(\partial^\alpha K)N^{*\mu} + \frac{ig_2}{m_K^2}\bar{\Lambda}^*_\mu\gamma_5\left(\partial^\mu\partial_\nu K\right)N^{*\nu} + \text{h.c.}, \tag{4}$$

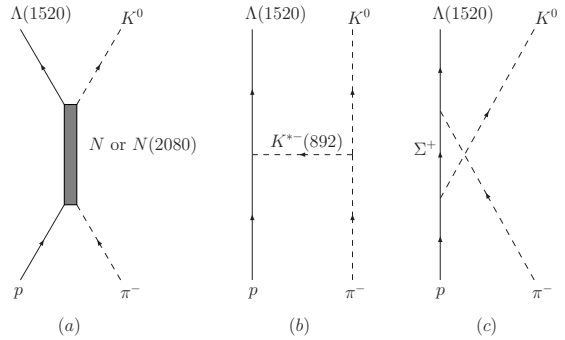

FIG. 1. Feynman diagrams for $\pi^- p \to K^0\Lambda(1520)$ reaction. The contributions from $t-$channel K^* exchange, $u-$channel Σ^+ exchange, and $s-$channel nucleon pole and $N^*(2080)$ resonance are considered.

for the $s-$channel neutron pole and $N^*(2080)$ processes, and

$$\mathcal{L}_{K^*N\Lambda^*} = ig_{K^*N\Lambda^*}\bar{\Lambda}^{*\mu}K^*_\mu N + \text{h.c.}, \tag{5}$$

$$\mathcal{L}_{K^*K\pi} = g_{K^*K\pi}[\bar{K}(\partial^\mu\vec{\tau}\cdot\vec{\pi})K^*_\mu - (\partial^\mu\bar{K})\vec{\tau}\cdot\vec{\pi}K^*_\mu] + \text{h.c.}, \tag{6}$$

for the $t-$channel K^* exchange process, while

$$\mathcal{L}_{KN\Sigma} = -ig_{KN\Sigma}\bar{N}\gamma_5 K\vec{\tau}\cdot\vec{\Sigma} + \text{h.c.}, \tag{7}$$

$$\mathcal{L}_{\pi\Sigma\Lambda^*} = \frac{g_{\pi\Sigma\Lambda^*}}{m_\pi}\bar{\Lambda}^{*\mu}\gamma_5(\partial_\mu\vec{\pi}\cdot\vec{\Sigma}) + \text{h.c.}, \tag{8}$$

for the $u-$channel Σ exchange diagram.

The above Lagrangian densities are also used to study the contributions of the terms shown in Fig. 2 for $pp \to pK^+\Lambda(1520)$ reaction.

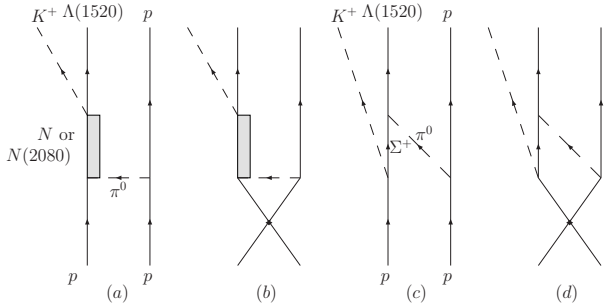

FIG. 2. Feynman diagrams for $pp \to pK^+\Lambda(1520)$ reaction. The diagram (a) and (c) show the direct processes, while (b) and (d) show the exchange processes.

It is worth to note that we use the Rarita-Schwinger formalism [25, 26] to describe the spin $J = 3/2$ $\Lambda(1520)$ and $N^*(2080)$ resonances, while the $\Lambda(1520)$ and $N^*(2080)$ hadronic couplings will be discussed in the following section.

B. Coupling constants and form factors

Firstly, the coupling constant for πNN vertex is taken to be $g_{\pi NN} = 13.45$, and the coupling constant $g_{KN\Sigma}$

is taken as 2.69 from SU(3) symmetry. While the $N^*(2080)\Lambda(1520)K$ coupling constants $g_{1,2}$ are taken as the values that we have obtained in Ref. [13], with the values $g_1 = 1.4$ and $g_2 = 5.5$. The $\Lambda^* NK^*$ vertex shown in Eq. (6) is predominantly $s-$wave, and the value of its coupling constant, $g_{K^*N\Lambda^*}$, is 0.5, which was obtained and used in Ref. [16] (see more details about the $\Lambda^* NK^*$ couplings in that reference).

Secondly, the coupling constants, $g_{\Lambda^* KN}$, $g_{K^* K\pi}$, and $g_{\Lambda^*\pi\Sigma}$, are determined from the experimentally observed partial decay widths of the $K^* \to K\pi$, $\Lambda(1520) \to KN$, and $\Lambda(1520) \to \pi\Sigma$, respectively. With the effective interaction Lagrangians described by Eq. (2), Eq. (6), and Eq. (8), the partial decay widths $\Gamma_{\Lambda(1520)\to KN}$, $\Gamma_{K^*\to K\pi}$, and $\Gamma_{\Lambda(1520)\to\pi\Sigma}$, can be easily calculated. The coupling constants are related to the partial decay widths as,

$$\Gamma_{\Lambda(1520)\to KN} = \frac{g^2_{\Lambda^* KN}}{6\pi}\frac{|\overrightarrow{p^{\rm c.m.}_N}|^3(E_N - m_N)}{m^2_K M_{\Lambda^*}}, \quad (9)$$

$$\Gamma_{K^*\to K\pi} = \frac{g^2_{K^* K\pi}}{2\pi}\frac{|\overrightarrow{p^{\rm c.m.}_\pi}|^3}{m^2_{K^*}}, \quad (10)$$

$$\Gamma_{\Lambda(1520)\to\pi\Sigma} = \frac{g^2_{\Lambda^*\pi\Sigma}}{4\pi}\frac{|\overrightarrow{p^{\rm c.m.}_\Sigma}|^3(E_\Sigma - m_\Sigma)}{m^2_\pi M_{\Lambda^*}}, \quad (11)$$

where

$$E_{N/\Sigma} = \frac{M^2_{\Lambda^*} + m^2_{N/\Sigma} - m^2_{K/\pi}}{2M_{\Lambda^*}}, \quad (12)$$

and

$$|\overrightarrow{p^{\rm c.m.}_{N/\Sigma}}| = \sqrt{E^2_{N/\Sigma} - m^2_{N/\Sigma}}, \quad (13)$$

$$|\overrightarrow{p^{\rm c.m.}_\pi}| = \frac{\sqrt{[m^2_{K^*} - (m_K + m_\pi)^2][m^2_{K^*} - (m_K - m_\pi)^2]}}{2m_{K^*}}. \quad (14)$$

With mass ($M_{\Lambda^*} = 1519.5$ MeV, $m_{K^*} = 893.1$ MeV), total decay width ($\Gamma_{\Lambda^*} = 15.6$ MeV, $\Gamma_{K^*} = 49.3$ MeV), and decay branching ratios of $\Lambda(1520)$ [$\mathrm{Br}(\Lambda^* \to KN) = 0.45 \pm 0.01$, $\mathrm{Br}(\Lambda^* \to \pi\Sigma) = 0.42 \pm 0.01$] and K^* [$\mathrm{Br}(K^* \to K\pi) \sim 1$], we obtain these coupling constants as listed in Table I.

Finally, the strong coupling constant $g_{N^*N\pi}$ is a free parameter, which will be obtained by fitting it to the total cross sections of $\pi^- p \to K^0\Lambda(1520)$ reaction.

Since the hadrons are not point like particles, we ought to introduce the compositeness of the hadrons. This is usually achieved by including the relevant off shell form factors in the amplitudes. There is no unique theoretical way to introduce the form factors, and this was discussed at length in the late nineties [27–30]. We adopt here the common scheme used in many previous works,

$$f_i = \frac{\Lambda^4_i}{\Lambda^4_i + (q^2_i - M^2_i)^2}, \quad i = s, t, u, R \quad (15)$$

$$\text{with} \quad \begin{cases} q^2_s = q^2_R = s,\ q^2_t = t,\ q^2_u = u, \\ M_s = m_N,\ M_{\rm R} = M_{N^*}, \\ M_{\rm u} = m_\Sigma, \\ M_{\rm t} = m_{K^*}, \end{cases} \quad (16)$$

where s, t and u are the Lorentz-invariant Mandelstam variables. In the present calculation, $q_s = q_R = p_1 + p_2$, $q_t = p_1 - p_3$, and $q_u = p_4 - p_1$ are the 4-momentum of intermediate nucleon pole and $N^*(2080)$ in the $s-$channel, exchanged K^* meson in the $t-$chanel, and exchanged Σ in the $u-$channel, respectively. While p_1, p_2, p_3 and p_4 are the 4-momenta for π^-, p, K^0 and $\Lambda(1520)$, respectively. Besides, we will consider different cut-off values for the background and resonant terms, i.e. $\Lambda_s = \Lambda_t = \Lambda_u \neq \Lambda_R$.

For $pp \to pK^+\Lambda(1520)$ reaction, we also need the relevant off-shell form factors for πNN and πNN^* vertexes. We take them as

$$F^{NN}_\pi(k^2_\pi) = \frac{\Lambda^2_\pi - m^2_\pi}{\Lambda^2_\pi - k^2_\pi}, \quad (17)$$

$$F^{N^*N}_\pi(k^2_\pi) = \frac{\Lambda^{*2}_\pi - m^2_\pi}{\Lambda^{*2}_\pi - k^2_\pi}, \quad (18)$$

with k_π the 4-momentum of the exchanged π meson. The cutoff parameters are taken as $\Lambda_\pi = \Lambda^*_\pi = 1.3$ GeV as used in Ref. [24].

TABLE I. Values of the coupling constants required for the estimation of the $\pi^- p \to K^0\Lambda(1520)$ and $pp \to pK^+\Lambda(1520)$ reactions. These have been estimated from the decay branching ratios quoted in the PDG book [2], though it should be noted that these are for all final charged state.

Decay modes	Adopted branching ratios	$g^2/4\pi$ [a]
$\Lambda^* \to KN$	0.45	8.77
$\Lambda^* \to \pi\Sigma$	0.42	0.02
$K^* \to K\pi$	1.00	0.84

[a] It should be stressed that the partial decay width determine only the square of the corresponding coupling constants as shown in Eqs. (9, 10, 11), thus their signs remain uncertain. Predictions from quark model can be used to constrain these signs. Unfortunately, quark model calculations for these vertices are still sparse. So, in the present calculation, we choose a positive sign for these results.

C. Scattering amplitudes

For the $\pi^- p \to K^0\Lambda(1520)$ reaction, with the effective interaction Lagrangian densities given above, we can easily construct the invariant scattering amplitudes,

$$-iT_i = \bar{u}_\mu(p_4, s_{\Lambda^*})A^\mu_i u(p_2, s_p), \quad (19)$$

where u_μ and u are dimensionless Rarita-Schwinger and Dirac spinors, respectively, while s_{Λ^*} and s_p are the spin polarization variables for final $\Lambda(1520)$ resonance and initial proton, respectively. To get the scattering amplitude, we also need the propagators for nucleon and $N^*(2080)$, K^* meson, and Σ^+ baron,

$$G_N(q_s) = i\frac{\not{q}_s + m_N}{s - m_N^2}, \tag{20}$$

$$G^{\mu\nu}_{K^*}(q_t) = i\frac{-g^{\mu\nu} + q_t^\mu q_t^\nu}{t - m^2_{K^*}}, \tag{21}$$

$$G_\Sigma(q_u) = i\frac{\not{q}_u + m_\Sigma}{u - m^2_\Sigma}, \tag{22}$$

$$G^{\mu\nu}_{N^*}(q_R) = i\frac{\not{q}_R + M_{N^*}}{s - M^2_{N^*} + iM_{N^*}\Gamma_{N^*}}P^{\mu\nu}, \tag{23}$$

and

$$P^{\mu\nu} = -g^{\mu\nu} + \frac{1}{3}\gamma^\mu\gamma^\nu + \frac{2}{3M^2_{N^*}}q_R^\mu q_R^\nu + \frac{1}{3M_{N^*}}(\gamma^\mu q_R^\nu - \gamma^\nu q_R^\mu), \tag{24}$$

where M_{N^*} and Γ_{N^*} are the mass and the total decay width of the N^* resonance.

Then, the reduced A_i^μ amplitudes in Eq. (19) can be easily obtained,

$$A_s^\mu = -i\frac{\sqrt{2}g_{\pi NN}g_{KN\Lambda^*}}{m_K(s - m_n^2)}(\not{q}_s - m_n)\gamma_5 p_3^\mu f_s, \tag{25}$$

$$A_t^\mu = -i\frac{\sqrt{2}g_{K^*K\pi}g_{K^*N\Lambda^*}}{t - m^2_{K^*}}(p_1^\mu + p_3^\mu - \frac{m_K^2 - m_\pi^2}{m^2_{K^*}}q_t^\mu)f_t, \tag{26}$$

$$A_u^\mu = -i\frac{\sqrt{2}g_{\pi\Sigma\Lambda^*}g_{KN\Sigma}}{m_\pi(u - m^2_{\Sigma^+})}(\not{q}_u - m_{\Sigma^+})p_1^\mu f_u, \tag{27}$$

$$A_R^\mu = i\frac{\sqrt{2}g_{\pi NN^*}}{m_\pi m_K D}\Big[g_1\not{p}_3(\not{q}_R - M_{N^*})\Big(p_1^\mu - \frac{1}{3}\gamma^\mu\not{p}_1 + \frac{1}{3M_{N^*}}(\gamma^\mu q_R\cdot p_1 - q_R^\mu\not{p}_1) - \frac{2}{3M^2_{N^*}}q_R^\mu q_R\cdot p_1\Big) + \frac{g_2}{m_K}(\not{q}_R - M_{N^*})p_3^\mu\Big(p_1\cdot p_3 - \frac{1}{3}\not{p}_3\not{p}_1 + \frac{1}{3M_{N^*}}(\not{p}_3 q_R\cdot p_1 - q_R\cdot p_3\not{p}_1) - \frac{2}{3M^2_{N^*}}q_R\cdot p_3 q_R\cdot p_1\Big)\Big]f_R, \tag{28}$$

with the sub-indices s, t, u and R stand for the $s-$channel nucleon pole, $t-$channel K^* exchange, $u-$channel Σ^+ exchange, and resonance $N^*(2080)$ terms.

For the $pp \to pK^+\Lambda$ reaction, the full invariant amplitude in our calculation is composed of four parts corresponding to the $s-$channel nucleon pole and $N^*(2080)$ resonance, $t-$chanel K^*, and $u-$channel Σ, which are produced by the π^0-meson exchanges, respectively,

$$\mathcal{M} = \sum_{i=s,\ t,\ u,\ R}\mathcal{M}_i. \tag{29}$$

Each of the above amplitudes can be obtained straightforwardly with the effective couplings and following the Feynman rules. Here we give explicitly the amplitude $\mathcal{M}_s$, as an example,

$$\mathcal{M}_s = \frac{g^2_{\pi NN}g_{\Lambda^*KN}}{m_K}F_\pi^{NN}(k_\pi^2)F_\pi^{N^*N}(k_\pi^2)F_s(q_N^2)G_\pi(k_\pi^2)\times \bar{u}_\mu(p_4,s_4)p_5^\mu\gamma_5 G_N(q_N)u(p_1,s_1)\bar{u}(p_3,s_3)\gamma_5 u(p_2,s_2) + (\text{exchange term with } p_1 \leftrightarrow p_2), \tag{30}$$

where s_i $(i = 1, 2, 3)$ and p_i $(i = 1, 2, 3)$ represent the spin projection and 4-momenta of the two initial and one final protons, respectively. While p_4 and p_5 are the 4-momenta of the final $\Lambda(1520)$ and K meson, respectively. And s_4 stands the spin projection of $\Lambda(1520)$. In Eq. (30), $k_\pi = p_2 - p_3$ and $q_N = p_4 + p_5$ stand for the 4-momenta of the exchanged π meson and intermediate nucleon. And $G_\pi(k_\pi)$ is the pion meson propagator,

$$G_\pi(k_\pi) = \frac{i}{k_\pi^2 - m_\pi^2}. \tag{31}$$

D. Cross sections for $\pi^- p \to K^0\Lambda(1520)$ reaction

The differential cross section for $\pi^- p \to K^0\Lambda(1520)$ reaction at center of mass (c.m.) frame can be expressed as

$$\frac{d\sigma}{d\cos\theta} = \frac{1}{32\pi s}\frac{|\vec{p_3}^{\,\text{c.m.}}|}{|\vec{p_1}^{\,\text{c.m.}}|}\left(\frac{1}{2}\sum_{s_{\Lambda^*},s_p}|T|^2\right), \tag{32}$$

where θ denotes the angle of the outgoing K^0 relative to beam direction in the c.m. frame, while $\vec{p_1}^{\,\text{c.m.}}$ and $\vec{p_3}^{\,\text{c.m.}}$ are the 3-momentum of the initial π^- and final K^0 mesons. The total invariant scattering amplitude T is given by,

$$T = T_s + T_t + T_u + T_R\,. \tag{33}$$

From the amplitude, we can easily obtain the total cross sections of the $\pi^- p \to K^0\Lambda(1520)$ reaction as functions of the invariant mass of $\pi^- p$ system. We perform three parameter ($g_{N^*N\pi}$, $\Lambda_s = \Lambda_t = \Lambda_u$ and Λ_R) χ^2-fits to the experimental data [31] on total cross sections for $\pi^- p \to K^0\Lambda(1520)$ reaction. There is a total of 12 data points below $\sqrt{s} = 3.1$ GeV.

The fitted parameters are: $g_{N^*N\pi} = 0.14 \pm 0.04, \Lambda_s = \Lambda_t = \Lambda_u = 0.89 \pm 0.05$ and $\Lambda_R = 0.91 \pm 0.03$. The resultant χ^2/dof is 1.1. The best fitting results for the total cross sections are shown in Fig. 3, comparing with the data. The solid lines represent the full results, while the contributions from the $s-$channel nucleon pole, $t-$channel K^* exchange, $u-$channel Σ^* and $s-$channel $N^*(2080)$ terms are shown by the dashed, dotted, dot-dashed, and dash-dot-dotted lines, respectively. From Fig. 3, one can see that we can describe the experimental data of total cross sections quite well, while the

$s-$channel nucleon pole and $N^*(2080)$ resonance and also the $u-$channel Σ exchange give the dominant contributions below $\sqrt{s} = 2.4$ GeV. The $t-$channel K^* exchange diagram gives the minor contribution.

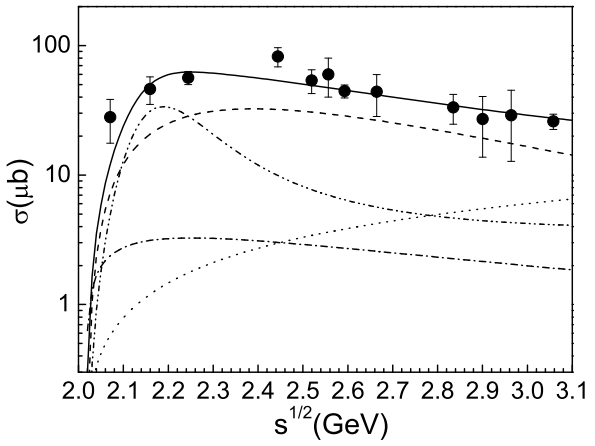

FIG. 3. Total cross sections vs the invariant mass $s^{\frac{1}{2}}$ for $\pi^- p \to K^0\Lambda(1520)$ reaction. The experimental data are from Ref. [31]. The curves are the contributions from $s-$channel nucleon pole term (dashed), $t-$channel K^* term (dotted), $u-$channel Σ term (dash-dotted), $s-$channel $N^*(2080)$ term (dash-dot-dotted) and the total contributions of them (solid).

With the above fitted parameters, the corresponding calculation results for the differential cross sections for $\pi^- p \to K^0\Lambda(1520)$ reaction at the energy around the central mass of $N^*(2080)$ resonance, $\sqrt{s} = 2.05$ GeV, $\sqrt{s} = 2.10$ GeV, and $\sqrt{s} = 2.15$ GeV, are shown in Fig 4, by which the future experiments can check our model.

On the other hand, with the strong coupling constant, $g_{N^*N\pi}$, which was obtained from the χ^2-fits, we have evaluated the $N^*(2080)$ resonnance to $N\pi$ partial decay width,

$$\Gamma_{N^*\to N\pi} = \frac{g^2_{N^*N\pi}}{4\pi}\frac{|\vec{p}^{\,\rm c.m.}_N|^3}{m^2_\pi M_{N^*}}(E_N - m_N), \qquad (34)$$

as deduced from the Lagrangian density of Eq. (3). In the above expression,

$$E_N = \frac{M^2_{N^*} + m^2_N - m^2_\pi}{2M_{N^*}}, \qquad (35)$$

$$|\vec{p}^{\,\rm c.m.}_N| = \sqrt{E^2_N - m^2_N}. \qquad (36)$$

With the values of $M_{N^*} = 2115$ MeV, $\Gamma_{N^*} = 254$ MeV, and also $g_{N^*N\pi} = 0.14 \pm 0.04$ we can get

$$\mathrm{Br}(N^* \to N\pi) = \frac{\Gamma_{N^*\to N\pi}}{\Gamma_{N^*}} = (2.9 \pm 1.6)\%, \qquad (37)$$

with the error from the uncertainty of the coupling constant $g_{N^*N\pi}$. The above value is consistent with the result $(6 \pm 2)\%$ that was obtained from the multichannel analysis [32].

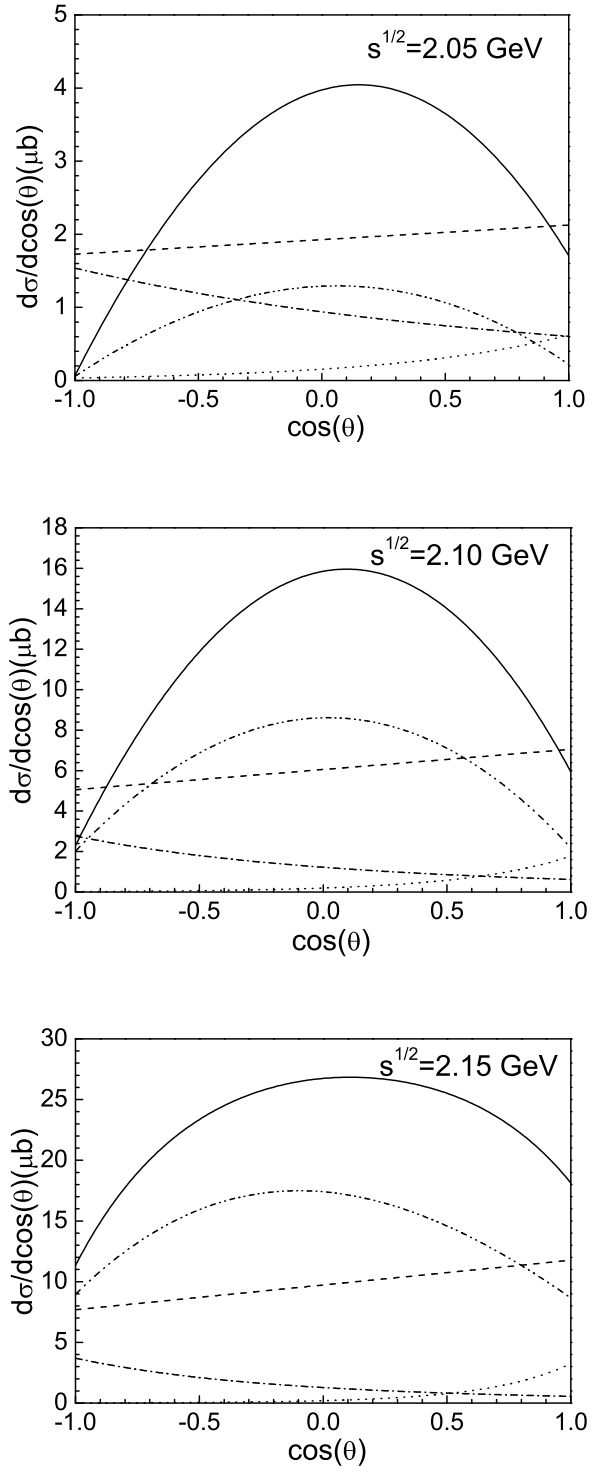

FIG. 4. Differential cross sections for $\pi^- p \to K^0\Lambda(1520)$ reaction at $\sqrt{s} = 2.05$ GeV, $\sqrt{s} = 2.10$ GeV, and $\sqrt{s} = 2.15$ GeV. The curves are the contributions from $s-$channel nucleon pole term (dashed), $t-$channel K^* term (dotted), $u-$channel Σ term (dash-dotted), $s-$channel $N^*(2080)$ term (dash-dot-dotted) and the total contributions of them (solid).

III. NUMERICAL RESULTS FOR $pp \to pK^+\Lambda(1520)$ REACTION AND DISCUSSIONS

With the formalism and ingredients given above, the calculations of the differential and total cross sections for $pp \to pK^+\Lambda(1520)$ are straightforward,

$$d\sigma(pp \to pK^+\Lambda(1520)) = \frac{1}{4}\frac{m_p^2}{F}\sum_{s_1,s_2}\sum_{s_3,s_4}|\mathcal{M}|^2 \times \frac{m_p d^3p_3}{E_3}\frac{m_{\Lambda(1520)}d^3p_4}{E_4}\frac{d^3p_5}{2E_5}\delta^4(p_1+p_2-p_3-p_4-p_5), \tag{38}$$

with the flux factor

$$F = (2\pi)^5\sqrt{(p_1\cdot p_2)^2 - m_p^4}\ . \tag{39}$$

With the formalism and ingredients given above, the total cross section versus the beam energy (p_{lab}) of the proton for the $pp \to pK^+\Lambda(1520)$ reaction is calculated by using a Monte Carlo multi-particle phase space integration program. The results for beam energies p_{lab} from just above the production threshold 3.59 GeV to 5.0 GeV are shown in Fig. 5. The dashed, dotted, and dash-dotted lines stand for contributions from nucleon pole, Σ pole and $N^*(2080)$ resonance, respectively. Their total contributions are shown by the solid line. [2] From Fig. 5, we can see that the contribution from the $u-$channel Σ exchange is predominant at the very close to threshold region, but, when the beam energy goes up, the contributions from $s-$channel nucleon pole and $N^*(2080)$ resonance turn to be very important.

It is important to note that our predictions for the total cross section of $pp \to pK^+\Lambda(1520)$ reaction, at $p_{lab} = 3.65$ GeV, is $0.01\mu b$, which is 20 times smaller than the experimental upper limit $0.2\mu b$ as measured by the COSY-ANKE Collaboration [9]. This shows that our model predictions are consistent with the experimental results. Moreover, the total cross section of $pp \to pK^+\Lambda(1520)$ reaction is measured with HADES [34] at GSI at kinetic beam energy $T_p = 3.5$ GeV (corresponding to $p_{lab} = 4.34$ GeV)[3]. The result is $5.6 \pm 1.1 \pm 0.4^{+1.1}_{-1.6}$ μb, as shown in Fig. 5, by comparing with our theoretical result, 11.5 μb. If we modify the cut off parameters Λ_π and Λ_π^* from 1.3 GeV to 1.0 GeV, we get $\sigma = 5.45$ μb, which is in agreement with the experimental data well. However, it does not make sense to fit the only one data point. So we still take $\Lambda_\pi = \Lambda_\pi^* = 1.3$ GeV as used in many previous works [24]. We should also mention that, in the present calculation, we did not include the $\Lambda(1520)p$ final-state-interaction (FSI), which can increase the results even by a factor of 10 at the very near threshold region, such as the important role played by Λp FSI in the $pp \to pK^+\Lambda$ reaction [33]. This is because there are no experimental data on this reaction and also very scarce information about the $\Lambda(1520)p$ FSI.

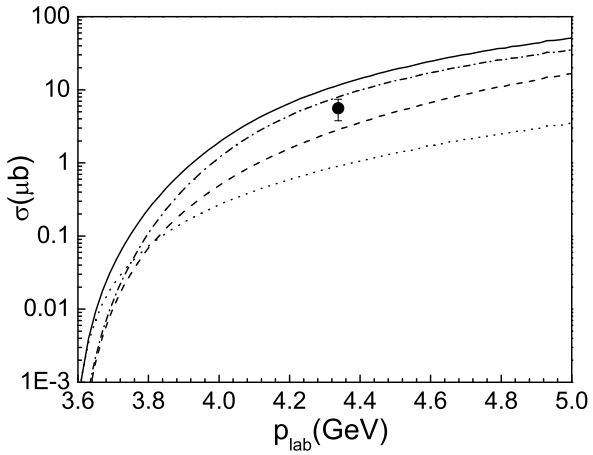

FIG. 5. Total cross sections vs beam energy p_{lab} of proton for the $pp \to pK^+\Lambda(1520)$ reaction from present calculation. The dashed, dotted, and dash-dotted lines stand for contributions from nucleon pole, Σ pole and $N^*(2080)$ resonance, respectively. Their total contribution are shown by the solid line. The one data point is taken from Ref. [34] is also shown.

Furthermore, the corresponding momentum distribution of the final proton and K^+ meson, the $K\Lambda(1520)$ invariant mass spectrum, and also the Dalitz Plot for the $pp \to pK^+\Lambda(1520)$ reaction at beam momentum $p_{lab} = 3.67$ GeV, which is reachable for DISTO Collaboration [5], are calculated and shown in Fig. 6. [4] The dashed lines are pure phase space distributions, while, the solid lines are full results from our model. From Fig. 6, we can see that even at $p_{lab} = 3.67$ GeV, there is a clear bump in the $K\Lambda(1520)$ invariant mass distribution, which is produced by including the contribution from $N^*(2080)$ resonance.

At the energy point of beam momentum $p_{lab} = 3.67$ GeV, the contribution from $u-$channel Σ exchange is still dominant, so, for comparing, we also present our calculated differential distributions at $p_{lab} = 4.34$ GeV where the contribution from the $s-$channel nucleon pole and $N^*(2080)$ resonance is dominant. Our results are shown in Fig. 7. We can see that our model results for the momentum distribution of final proton are much different from the phase space distribution.

[2] Since the $t-$channel K^* meson exchange gives very small contribution to the $\pi^- p \to K^0\Lambda(1520)$ reaction, especially for the invariant mass of $K\Lambda(1520)$ below 2.4 GeV, so in the calculation for $pp \to pK^+\Lambda(1520)$ reaction, we ignore the contribution from it.

[3] $p_{lab} = \sqrt{{E_{lab}}^2 - m_p^2} = \sqrt{(T_p + m_p)^2 - m_p^2}$.

[4] It is worth to note that our results are calculated in the reaction laboratory frame, in which the target proton is at rest.

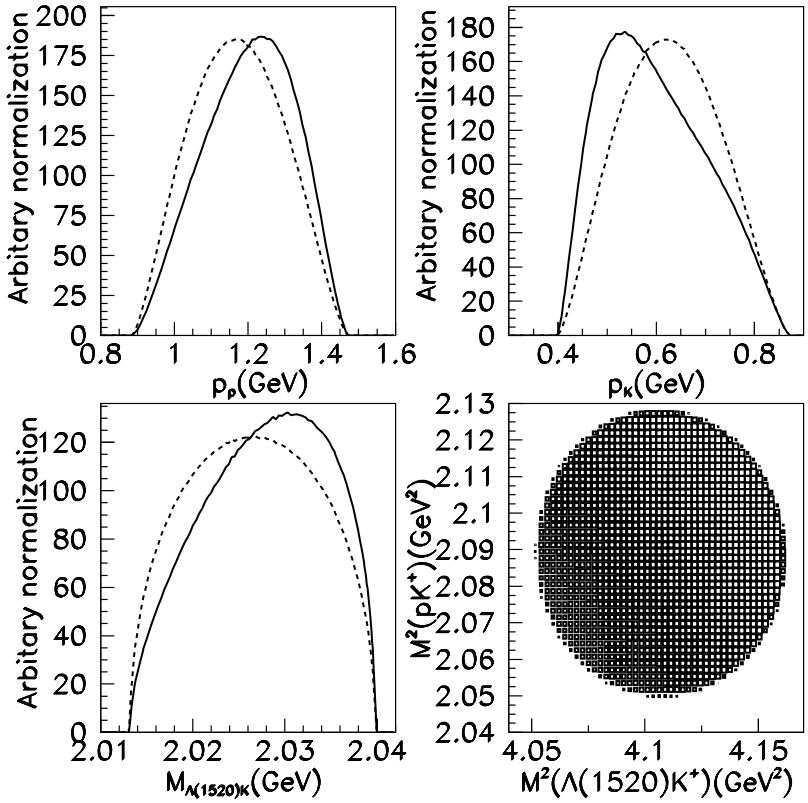

FIG. 6. Momentum distribution, invariant mass spectrum, and Dalitz Plot for the $pp \to pK^+\Lambda(1520)$ reaction at beam energy $p_{lab} = 3.67$ GeV comparing with the phase space distribution.The dashed lines are pure phase space distributions, while, the solid lines are full results from our model.

The momentum distribution, invariant mass spectra and the Dalitz plots in Figs. 6 and 7 show direct information about the $pp \to pK^+\Lambda(1520)$ reaction mechanism and may be tested by the future experiments.

IV. SUMMARY

In this paper, the $\Lambda(1520)$ hadronic production in proton-proton and $\pi^- p$ collisions are studied within the combination of the effective Lagrangian approach and the isobar model. For $\pi^- p \to K^0\Lambda(1520)$ reaction, in addition to the "background" contributions from $t-$channel K^* exchange, $u-$channel Σ^+ exchange, and $s-$channel nucleon pole terms, we also considered the contribution from the nucleon resonance $N^*(2080)$ (spin-parity $J^P = 3/2^-$), which has significant coupling to $K\Lambda(1520)$ channel. We show that the inclusion of the nucleon resonance $N^*(2080)$ leads to a fairly good description of the low energy experimental total cross section data of $\pi^- p \to K^0\Lambda(1520)$ reaction. The $s-$channel nucleon pole and $N^*(2080)$ resonance and also the $u-$channel Σ exchange give the dominant contributions below invariant mass $\sqrt{s} = 2.4$ GeV, while the $t-$channel K^* exchange diagram gives the minor contribution.

From χ^2-fits to the available experimental data for the $\pi^- p \to K^0\Lambda(1520)$ reaction, we get the $N^*(2080)N\pi$ coupling constant $g_{N^*(2080)N\pi} = 0.14 \pm 0.04$, which gives the branching ration of $N^*(2080)$ resonance to $N\pi$ as $(2.9 \pm 1.6)\%$. Our result is consistent with the previous work. Besides, the corresponding predictions for the differential cross sections of $\pi^- p \to K^0\Lambda(1520)$ are also shown, by which the future experiments can check our model.

Basing on the study of $\pi^- p \to pK^+\Lambda(1520)$ reaction, we study the $pp \to pK^+\Lambda(1520)$ reaction with the assumption that the production mechanism is due to the π^0-meson exchanges. We give our predictions about total cross sections of this reaction. Our results show that the contribution from the $u-$channel Σ exchange is predominant at the very near threshold region, but, when the beam energy goes up, the contributions from $s-$channel nucleon pole and $N^*(2080)$ resonance turn to be very important. Furthermore, we also demonstrate that the invariant mass distribution and the Dalitz Plot provide direct information of the $pp \to pK^+\Lambda(1520)$ reaction mechanisms and may be tested by the future experiments.

Finally, we would like to stress that due to the important role played by the resonant contribution in the $\pi^- p \to K^0\Lambda(1520)$ and $pp \to pK^+\Lambda(1520)$ reactions, accurate data for these reactions can be used to improve our knowledge on the $N^*(2080)$ properties, which are at

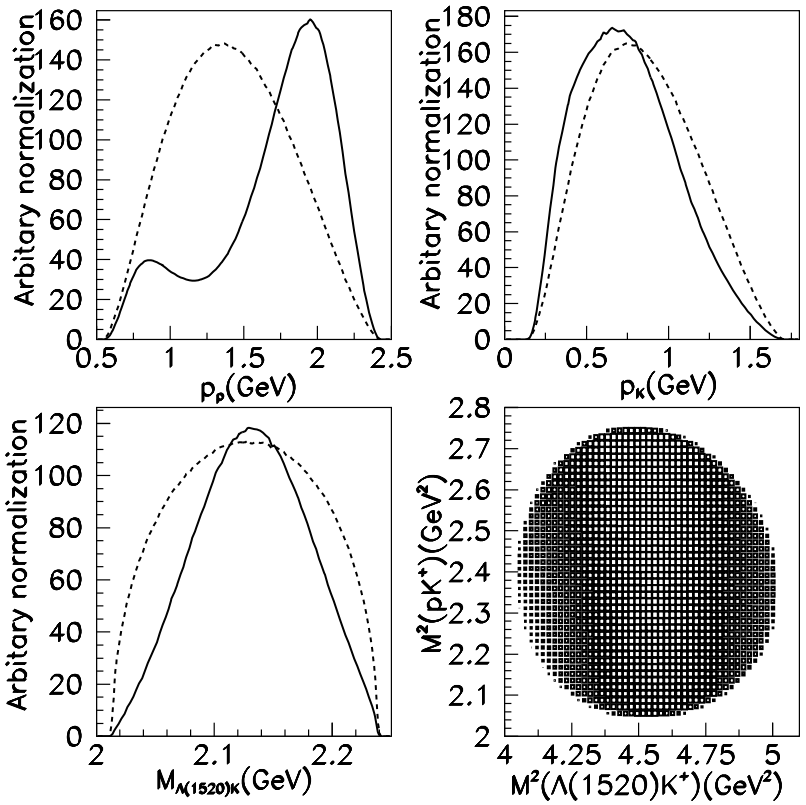

FIG. 7. As in Fig. 6, but for $p_{lab} = 4.34$ GeV

present poorly known. This work constitutes a first step in this direction.

ACKNOWLEDGMENTS

We would like to thank Prof. Bing-Song Zou for useful discussions and the CAS Theoretical Physics Center for Science Facilities for support and hospitality during the initiation of this work. This work is partly supported by the National Natural Science Foundation of China under grants 11105126 and 10905046.

[1] E. Klempt and J. M. Richard, Rev. Mod. Phys. **82**, 1095 (2010).
[2] J. Beringer et al., [Particel Data Group], Phys. Rev. D **86**, 010001 (2012).
[3] S. Capstick and W. Robert, Prog. Part. Nucl. Phys. **45**, S241 (2000), and references therein.
[4] B. S. Zou, eConf C **070910**, 112 (2007), and references therein.
[5] F. Balestra et al., Phys. Rev. C **63**, 024004 (2001).
[6] C. Quentmeier, H. H. Adam, J. T. Balewski, A. Budzanowski, D. Grzonka, L. Jarczyk, A. Khoukaz and K. Kilian *et al.*, Phys. Lett. B **515**, 276 (2001).
[7] P. Winter, M. Wolke, H. -H. Adam, A. Budzanowski, R. Czyzykiewicz, D. Grzonka, M. Janusz and L. Jarczyk *et al.*, Phys. Lett. B **635**, 23 (2006).
[8] M. Hartmann et al., Phys. Rev. Lett. **96**, 242301 (2006).
[9] I. Zychor et al., Phys. Lett. B **660**, 167 (2008).
[10] Y. Maeda et al., Phys. Rev. C **77**, 015204 (2008).
[11] L. S. Geng and E. Oset, Eur. Phys. J. A **34**, 405 (2007).
[12] J. J. Xie and C. Wilkin, Phys. Rev. C **82**, 025210 (2010).
[13] J. J. Xie and J. Nieves, Phys. Rev. C **82**, 045205 (2010).
[14] J. He and X. R. Chen, Phys. Rev. C **86**, 035204 (2012).
[15] Seung-il Nam, arXiv: 1212.6114.
[16] H. Toki, C. García-Recio, and J. Nieves, Phys. Rev. D **77**, 034001 (2008).
[17] F. Q. Wu, B. S. Zou, L. Li and D. V. Bugg, Nucl. Phys. A **735**, 111 (2004); F. Q. Wu, and B. S. Zou, Phys. Rev. D **73**, 114008 (2006).

[18] T. Feuster and U. Mosel, Phys. Rev. C **58**, 457 (1998); Phys. Rev. C **59**, 460 (1999); G. Penner and U. Mosel, Phys. Rev. C **66**, 055211 (2002); ibid. C **66**, 055212 (2002); V. Shklyar, H. Lenske and U. Mosel, Phys. Rev. C **72**, 015210 (2005).

[19] S. I. Nam, Phys. Rev. C **81**, 015201 (2010).

[20] B.S. Zou and F. Hussain, Phys. Rev. C **67**, 015204 (2003).

[21] K. Tsushima, S.W. Huang and A. Faessler, Phys. Lett. B **337**, 245 (1994); K. Tsushima, A. Sibirtsev and A.W. Thomas, Phys. Lett. B **39**, 29 (1997); K. Tsushima, A. Sibirtsev, A.W. Thomas and G.Q. Li, Phys. Rev. C **59**, 369 (1999), Erratum-ibid. C **61**, 029903 (2000).

[22] A. Sibirtsev and W. Cassing, nucl-th/9802019; A. Sibirtsev, K. Tsushima, W. Cassing and A. W. Thomas, Nucl. Phys. A **646**, 427 (1999).

[23] B. Julia-Diaz, B. Saghai, T.S.H. Lee and F. Tabakin, Phys. Rev. C **73**, 055204 (2006).

[24] J. -J. Xie, B. -S. Zou and B. -C. Liu, Chin. Phys. Lett. **22**, 2215 (2005); J. -J. Xie and B. -S. Zou, Phys. Lett. B **649**, 405 (2007); J. -J. Xie, B. -S. Zou and H. -C. Chiang, Phys. Rev. C **77**, 015206 (2008); B. -S. Zou and J. -J. Xie, Int. J. Mod. Phys. E **17**, 1753 (2008).

[25] W. Rarita and J. Schwinger, Phys. Rev. **60**, 61 (1941).

[26] L. M. Nath, B. Etemadi, and J. D. Kimel, Phys. Rev. D **3**, 2153 (1971).

[27] K. Ohta, Phys. Rev. C **40** (1989) 1335.

[28] H. Haberzettl, C. Bennhold, T. Mart, T. Feuster, Phys. Rev. C **58**, R40 (1998).

[29] R. M. Davidson and R. Workman, Phys. Rev. C **63**, 025210 (2001).

[30] S. Janssen, J. Ryckebusch, D. Debruyne and T. Van Cauteren, Phys. Rev. C **65**, 015201 (2002).

[31] A. Baldini, V. Flamino, W.G. Moorhead and D.R.O. Morrison, *Landolt-Börnstein*, *Numerical Data and Functional Relationships in Science an Technology*, vol.**12**, ed. by H. Schopper, Springer-Verlag(1988), *Total Cross Sections of High Energy Particles*.

[32] A. V. Anisovich et al., Eur. Phys. J. A **8**, 15 (2012).

[33] J. -J. Xie, H. -X. Chen and E. Oset, Phys. Rev. C **84**, 034004 (2011).

[34] G. Agakishiev *et al.*, [HADES Collaboration], arXiv: 1208.0205.